Probing Uniqueness of Equation of State of Neutron Stars

In the Next Generation of Gravitational Wave Detectors

Praveer Tiwari, Ajit K. Mehta, K.G Arun

Presented at the Finite-Temperature Effects in Multi-Messenger Astrophysics,
Institute for Nuclear Theory
June 19, 2026

Outline

Overview & Motivation

Why Does the EOS of Neutron Stars Matter?

- Neutron stars are the **densest stable objects** in the universe
- The equation of state $P(\mathcal{E})$ governs **structure, stability, and observables**
- Connects **nuclear physics**, and **QCD**, with neutron star characterization
- Characterization until now assumes the fact that the EoS of neutron stars are unique

Core question

Can we probe the presence of multiple population of neutron stars?

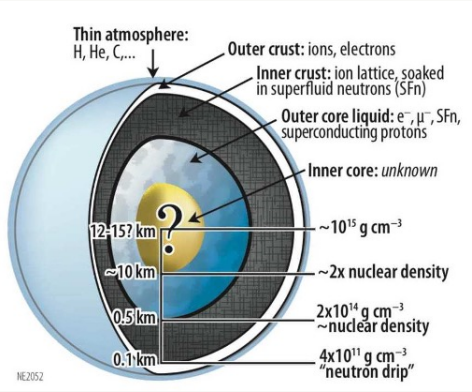

[a]Image Credit: https://heasarc.gsfc.nasa.gov/

Methodology

Heirarchical Bayesian Inference Framework

Pure Population - Gravitational Waves based Constraints

- Gravitational waves constrain tidal deformability $\tilde{\Lambda}$ of binary neutron stars.
- Constraints on EoS curve can be obtained by assuming an model for EoS and constraining model parameters, Υ_0^*
- The posterior on Υ_0 is then given by

$$p(\Upsilon_0 \mid \{d_i\}) \propto p(\{d_i\}, N_{\rm det} \mid \Upsilon_0) p(\Upsilon_0), \quad \text{where} \tag{1}$$

$$P(\{d_i\}, N_{\rm det} \mid \Upsilon_0) = \prod_{i=1}^{N} \int_{\tilde{\Lambda}, \mathcal{M}_i, q_i} \frac{P(\tilde{\Lambda}, \mathcal{M}_i, q_i \mid d_i)}{P_{PE}(\tilde{\Lambda}, M_i, q_i)} \frac{P(\tilde{\Lambda}, \mathcal{M}_i, q_i \mid \Upsilon_0)}{\xi(\Upsilon_0)} \, d\mathcal{M}_i \, dq_i \, d\tilde{\Lambda} \tag{2}$$

Extension to Mixed Population

- For multiple population of BNS, Υ_0 in the above equation gets replaced by $\{\Upsilon_p\} = \Upsilon_1 \cup \Upsilon_2 \cup \ldots \Upsilon_n$
- $P(\tilde{\Lambda}, \mathcal{M}_i, q_i \mid \{\Upsilon_p\})$ dictates what kind of population we want to mix

Two-Population Scenario

Decoding $P(\tilde{\Lambda}, \mathcal{M}_i, q_i \mid \{\Upsilon_p\})$

- If f is the fraction of vanilla (dominant) population, then

$$\begin{aligned} P(\tilde{\Lambda}, \mathcal{M}_i, q_i \mid \Upsilon) =& f\, P(\tilde{\Lambda}, \mathcal{M}_i, q_i \mid \Upsilon_1) + (1-f)\, P(\tilde{\Lambda}, \mathcal{M}_i, q_i \mid \Upsilon_2). \\ =& f\, P(\mathcal{M}_i, q_i \mid \Upsilon_1)\delta(\tilde{\Lambda} - \hat{\tilde{\Lambda}}_1(\mathcal{M}_i, q_i, \Upsilon_1)) + \\ & (1-f)\, P(\mathcal{M}_i, q_i \mid \Upsilon_2)\delta(\tilde{\Lambda} - \hat{\tilde{\Lambda}}_2(\mathcal{M}_i, q_i, \Upsilon_2)) \end{aligned} \tag{3}$$

$$\begin{aligned} P(\{d_i\}, N_{\rm det} \mid \Upsilon) = \frac{1}{\xi(\Upsilon)^{N_{\rm det}}} \prod_{i=1}^{N_{\rm det}} \int_{\mathcal{M}_i, q_i} & f \left(\frac{P(\hat{\tilde{\Lambda}}_1, \mathcal{M}_i, q_i \mid d_i)}{P_{PE}(\hat{\tilde{\Lambda}}_1, M_i, q_i)}\, P(\mathcal{M}_i, q_i \mid \Upsilon_1) \right) + \\ & (1-f) \left(\frac{P(\hat{\tilde{\Lambda}}_2, \mathcal{M}_i, q_i \mid d_i)}{P_{PE}(\hat{\tilde{\Lambda}}_2, M_i, q_i)}\, P(\mathcal{M}_i, q_i \mid \Upsilon_2) \right) d\mathcal{M}_i\, dq_i \end{aligned} \tag{4}$$

- $\hat{\tilde{\Lambda}}_1$ and $\hat{\tilde{\Lambda}}_2$ determines how tidal deformability depends on masses and Υ_i under specific theory/EoS

Two-Population Scenario (contd.)

Population simulated through two different EoS

- Assume that we have a Vanilla (Dominant) and Deviated EoS
- Vanilla EoS = APR4 (Modelled through piecewise polytrope) : $\{\log p_1, \Gamma_1, \Gamma_2, \Gamma_3\} = \{34.269, 2.830, 3.445, 3.348\}$
- Deviated EoS = APR4 but $\Gamma_2 = \delta\Gamma_2 + 3.445$
- $\Upsilon_1 = \{\Gamma_{2a}, \Gamma_3, f\}$, $\Upsilon_2 = \{\Gamma_{2b}, \Gamma_3, f\}$
- Γ_3, f are shared parameters

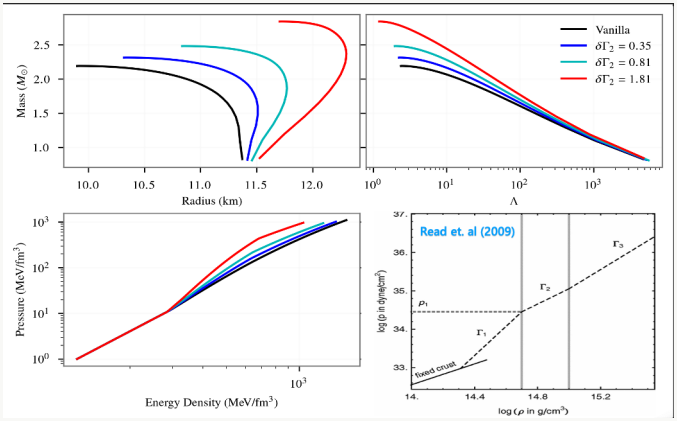

Injection Study

Injection in Cosmic Explorer Noise

Population Generation

- The masses are generated using power law model as mentioned in GWTC4
- Inclination angle $\sim$ cosine and luminosity distance is sampled assuming uniform comoving volume.

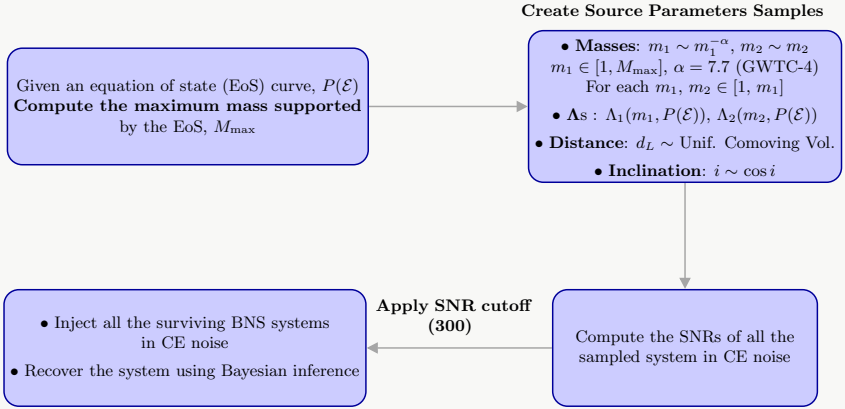

Injection in Cosmic Explorer Noise

Population Distribution ($\delta\Gamma_2 = 1.81$)

- The distributed masses are well separated
- SNR distribution indicated that the cutoff of 300 would produce $\sim$ 10 events

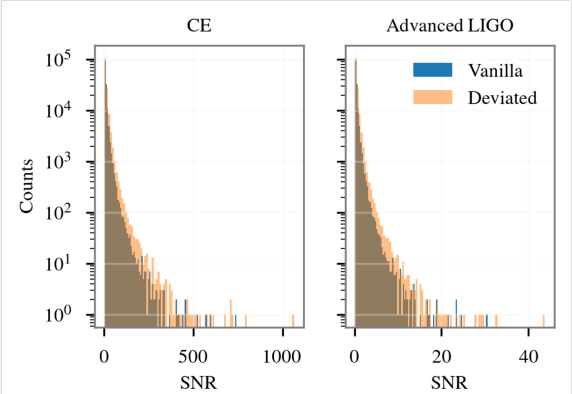

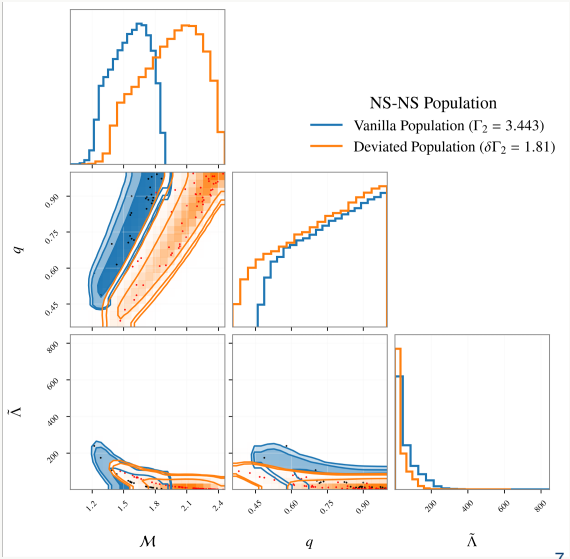

Results

Recovered EoS Parameters I

The Setup

- Prior Distributions: $\Gamma_{2a} \sim \mathcal{U}(2, 3.6)$, $\Gamma_{2b} \sim \mathcal{U}(3.6, 6)$, $\Gamma_3 \sim \mathcal{U}(1, 6)$, $f \sim \mathcal{U}(0, 1)$
- $\Gamma_{2,\mu} = f\Gamma_{2a} + (1-f)\Gamma_{2b}$; $\quad \delta\hat{\Gamma}_2 = \Gamma_{2,\mu} - \Gamma_{2a}$

Pure Population

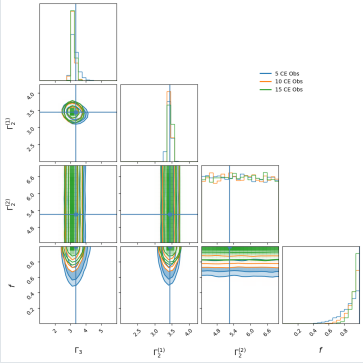

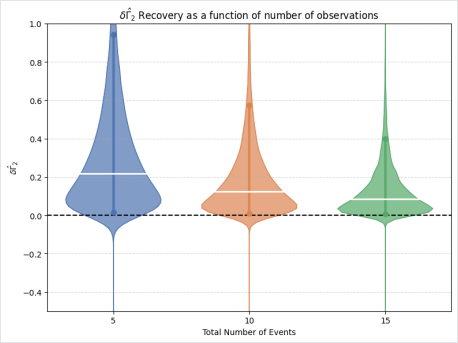

Recovered EoS Parameters II

Mixed Population with $\delta\Gamma_2 = 0.35$

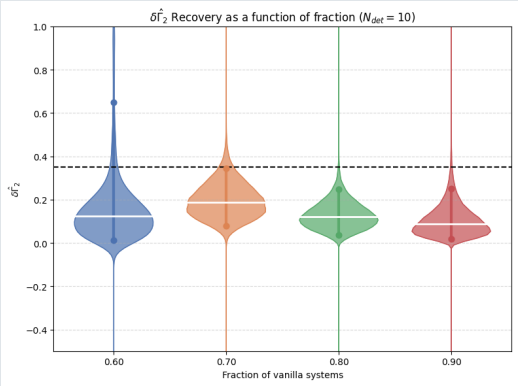

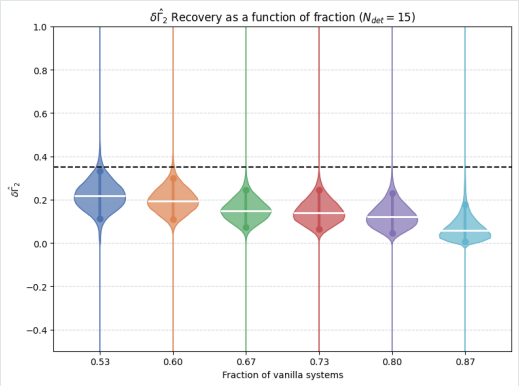

Recovered EoS Parameters III

Mixed Population with $\delta\Gamma_2 = 0.81$

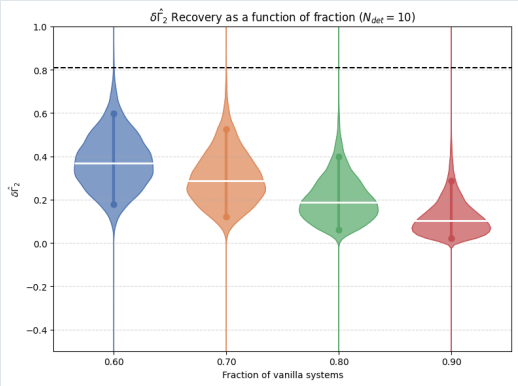

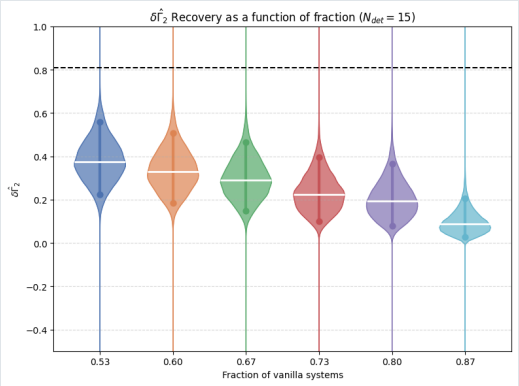

Recovered EoS Parameters IV - Overlapping Priors

The Setup

- Prior Distributions: $\Gamma_{2a} \sim \mathcal{U}(2, 4.25)$, $\Gamma_{2b} \sim \mathcal{U}(3.2, 6)$, $\Gamma_3 \sim \mathcal{U}(1, 6)$, $f \sim \mathcal{U}(0, 1)$
- $\delta\hat{\Gamma}_2 = \Gamma_{2b} - \Gamma_{2a}$

Mixed Population with $\delta\Gamma_2 = 0.81$

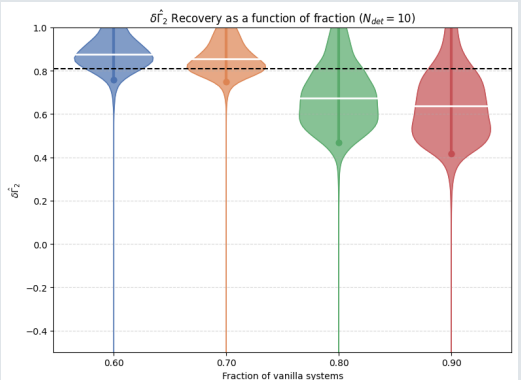

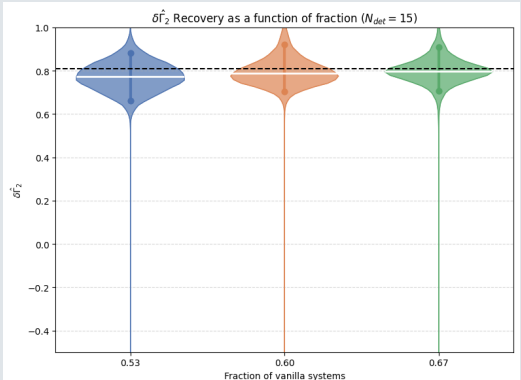

Recovered EoS Parameters V - Large Observations

Mixed Population with $\delta\Gamma_2 = 0.35$, $f = 0.8$

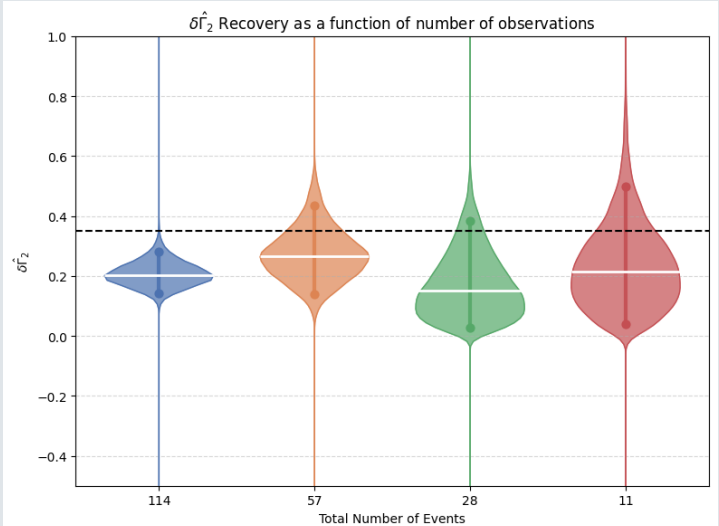

The Setup

- SNR Cutoff = 100
- Prior Distributions: $\Gamma_{2a} \sim \mathcal{U}(2, 3.6)$, $\Gamma_{2b} \sim \mathcal{U}(3.6, 6)$, $\Gamma_3 \sim \mathcal{U}(1, 6)$, $f \sim \mathcal{U}(0, 1)$
- $\Gamma_{2,\mu} = f\Gamma_{2a} + (1 - f)\Gamma_{2b}$; $\delta\hat{\Gamma}_2 = \Gamma_{2,\mu} - \Gamma_{2a}$

Summary

Summary

Deviation of $\delta\hat{\Gamma}_2$ from 0 imprints the information about mutiple BNS population. The accuracy of the value depends on

Number of Detected Events
We find that if $N_{det} > 10$ and if fraction of deviated population is greater than 0.2, we are able to confidently infer deviation.

Severity of Deviation
We find that for the low deviation of 0.35, it could take 15 observation, while for moderate deviation of 0.81, it takes 10 observations to confidently detect the deviation.

Nature of the Priors
Overlapping priors are more efficient in detecting the deviation as compared to disjoint priors.

Assumptions

- Working in source frame. Ignoring variation in cosmological params
- Outer regions of neutron stars are known
- Population parameters are fixed
- Injection in Gaussian noise
- Extrinsic parameters for GW detections are fixed
- Uncertainty in $\mathcal{M}$ and q is quite small

Thank you

Questions & Discussion

Backup: Updated Injection Framework

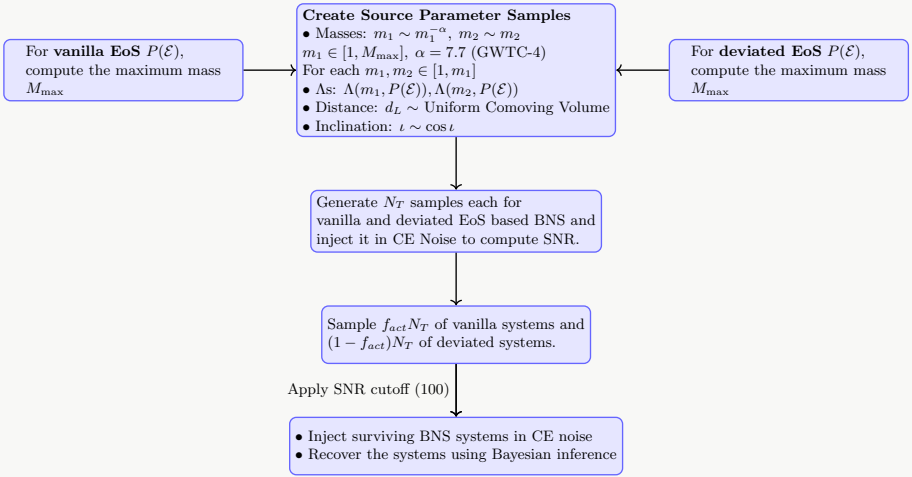

Backup: Mass Does Not Uniquely Fix Internal Structure

Gravitational mass is an *integral*:

$$M = 4\pi \int_0^R \varepsilon(r)\, r^2\, dr$$

Many density profiles $\varepsilon(r)$ integrate to the same M.

Fixed input		Unique output?
EOS + n_c	$\Rightarrow$	**Yes** — full structure
EOS + M	$\Rightarrow$	**No** — multiple branches
EOS + M + R	$\Rightarrow$	**Yes** — one point

This is why simultaneous M–R measurements (NICER) are so powerful.

The twin-star scenario

A strong first-order phase transition creates a **second stable branch** on the M–R curve [1, 2]. Two stars, same M, different R by 1–3 km — one hadronic, one hybrid/quark.

Backup: Beyond Twin Stars: Seven Mechanisms

1. **Thermal history**
   Young hot stars ($T \sim 10^{11}$ K) have thermal pressure support; age-matched stars of equal M are at different points in cooling [3].

2. **Rotation (spin)**
   Centrifugal support lowers central density. Spin-down raises n_c, potentially crossing phase thresholds. Same M, different $\Omega \Rightarrow$ different n_c [4].

3. **Magnetic field**
   Magnetars ($B \sim 10^{15}$ G) vs. MSPs ($B \sim 10^{8}$ G): Landau quantization shifts charged-particle fractions and hyperon onset density [5].

4. **Accretion history**
   Accreted matter spins up, buries B-field, and changes crust composition. Two stars at same final M may have started from different progenitor masses [6].

5. **Hyperon/kaon onset (crossover)**
   Hyperon fraction grows gradually above a threshold. Two stars straddling this threshold have qualitatively different core content despite similar M [7, 8].

6. **Dark matter admixture**
   DM accumulation rate depends on galactic position. Same total M can hide different baryonic fractions $\Rightarrow$ different nuclear n_c [9, 10].

7. **Non-equilibrium crust**
   Accreting systems (LMXBs) have crusts driven by pycnonuclear reactions out of catalyzed equilibrium — different nuclear species, heat capacity, and conductivity [6].

Backup:Multi-Messenger Observational Pillars

Gravitational Waves (LIGO/Virgo)

- GW170817 constrains tidal deformability $\tilde{\Lambda}$ [11, 12]
- Upper bound on pressure near $2n_0$ [12]
- GW190425 extends mass reach [13]

NICER X-ray Telescope

- Simultaneous M–R measurements via pulse-profile modelling [14, 15]
- PSR J0740+6620, J0030+0451, J0437−4715 [16–18]
- $R_{1.4} \approx 12$–$13\,\mathrm{km}$ [19]

Massive Pulsars (Radio)

- PSR J0740+6620: $M = 2.08\,M_\odot$ — requires stiff EOS [20]
- PSR J0952−0607: $M \approx 2.35\,M_\odot$ [21]
- Rules out most soft EOS models [22]

Lattice QCD (New 2025)

- First LQCD study of neutron-star interior [23]
- New bound on speed of sound c_s [23]
- Opens window to computational studies

Backup: EOS Uncertainty - Regime by Regime

Regime	n (fm^{-3})	Theory / Data	Pressure uncertainty
Outer crust	< 0.04	Nuclear structure	$\sim$ 10–15% [24]
Inner crust	0.04–0.16	χEFT, HIC	$\sim$ 20–30% [25]
Outer core	0.16–0.32	χEFT (N3LO)	factor ~ 2 [25, 26]
Inner core	0.32–0.64	NICER + GW (Bayesian)	factor ~ 5 [27]
Deep core	0.64–0.96	Max-mass constraint	factor $\sim$ 5–10 [19]
pQCD limit	$\gg 1.6$	Perturbative QCD	$\sim$ 10–20% [28]

Key quantitative result (2025)

Machine-learning + relativistic Brueckner-Hartree-Fock gives $P(5n_0) = 346.3 \pm 97.4\,\mathrm{MeV\,fm^{-3}}$ ($\approx 28\%$ fractional uncertainty from one method; full Bayesian envelope is wider) [29, 30].

Backup: TOV Equation

The Tolman–Oppenheimer–Volkoff equation is the relativistic hydrostatic equilibrium:

$$\frac{\mathrm{d}P}{\mathrm{d}r} = -\frac{\left[\varepsilon(r) + P(r)\right]\left[M(r) + 4\pi r^3 P(r)\right]}{r^2\left[1 - 2M(r)/r\right]}$$

where $M(r) = 4\pi \int_0^r \varepsilon(r')\, r'^2\, dr'$.

Given an EOS $P(\varepsilon)$ and central density n_c, the TOV system is integrated outward until $P = 0$, yielding M and R uniquely. **This is the sense in which the EOS, not the mass, is the fundamental input.**

Backup: Chiral EFT Breakdown

- χEFT is an expansion in p/Λ_b where $\Lambda_b \approx 500\,\text{MeV}$ is the breakdown scale
- At $n \sim 2n_0$, the Fermi momentum $k_F \sim 350\,\text{MeV}$ approaches Λ_b
- Higher-order many-body forces (3N, 4N) are poorly constrained
- Uncertainty grows exponentially: reliable at N^{3}LO below $\sim 2n_0$, unreliable above
- Bayesian methods (Gaussian Processes) propagate these correlated truncation errors to $P(n)$ and $c_s(n)$

Backup: Hyperon Puzzle

The puzzle:

- Hyperons (Λ, Σ, Ξ) are expected to appear at $n \sim 2$–$3n_0$
- Their onset softens the EOS (extra degrees of freedom reduce pressure)
- Most hyperonic EOS cannot support $M > 2\,M_\odot$
- Yet $2\,M_\odot$ stars are observed

Proposed resolutions:

- Repulsive hyperon three-body forces
- Quark deconfinement before hyperon onset
- In-medium mass modifications
- Modified vector-meson couplings

None is definitively established. The puzzle remains open.

References

[1] K. Schertler, C. Greiner, and M. H. Thoma. Medium Effects in Strange Quark Matter and the Equation of State. *Nuclear Physics A*, 616:659–679, 1997. doi: 10.1016/S0375-9474(97)00014-6.

[2] S. Benić, D. Blaschke, D. E. Alvarez-Castillo, T. Fischer, and S. Typel. A New Quark-Hadron Hybrid Equation of State for Astrophysics — I. High-Mass Twin Stars. *Astronomy & Astrophysics*, 577:A40, 2015. doi: 10.1051/0004-6361/201425318.

[3] D. Page, J. M. Lattimer, M. Prakash, and A. W. Steiner. Minimal Cooling of Neutron Stars: A New Paradigm. *Astrophysical Journal Supplement Series*, 155:623–650, 2004. doi: 10.1086/424844.

[4] E. Chubarian, H. Grigorian, G. S. Vartanyan, and D. Blaschke. Deconfinement Phase Transition in Rotating Nonspherical Compact Stars. *Astronomy & Astrophysics*, 357:968–976, 2000.

[5] A. Broderick, M. Prakash, and J. M. Lattimer. The Equation of State of Neutron Star Matter in Strong Magnetic Fields. *Astrophysical Journal*, 537:351–367, 2000. doi: 10.1086/309010.

[6] P. Haensel and J. L. Zdunik. Nuclear Composition and Heating in Accreted Neutron-Star Crusts. *Astronomy & Astrophysics*, 404:L33–L36, 2003. doi: 10.1051/0004-6361:20030521.

References ii

[7] D. Chatterjee and I. Vidaña. Do Hyperons Exist in the Interior of Neutron Stars? *European Physical Journal A*, 52:29, 2016. doi: 10.1140/epja/i2016-16029-x.

[8] D. B. Kaplan and A. E. Nelson. Strange Goings On in Dense Nucleonic Matter. *Physics Letters B*, 175:57–63, 1986. doi: 10.1016/0370-2693(86)90331-X.

[9] I. Goldman and S. Nussinov. Weakly Interacting Massive Particles and Neutron Stars. *Physical Review D*, 40:3221–3230, 1989. doi: 10.1103/PhysRevD.40.3221.

[10] A. de Lavallaz and M. Fairbairn. Neutron Stars as Dark Matter Probes. *Physical Review D*, 81:123521, 2010. doi: 10.1103/PhysRevD.81.123521.

[11] B. P. Abbott et al. GW170817: Observation of Gravitational Waves from a Binary Neutron Star Inspiral. *Physical Review Letters*, 119:161101, 2017. doi: 10.1103/PhysRevLett.119.161101.

[12] B. P. Abbott et al. GW170817: Measurements of Neutron Star Radii and Equation of State. *Physical Review Letters*, 121: 161101, 2018. doi: 10.1103/PhysRevLett.121.161101.

[13] B. P. Abbott et al. GW190425: Observation of a Compact Binary Coalescence with Total Mass $\sim 3.4\,M_{\odot}$. *Astrophysical Journal Letters*, 892:L3, 2020. doi: 10.3847/2041-8213/ab75f5.

[14] T. E. Riley et al. A NICER View of PSR J0030+0451: Millisecond Pulsar Parameter Estimation. *Astrophysical Journal Letters*, 887:L21, 2019. doi: 10.3847/2041-8213/ab481c.

References iii

[15] M. C. Miller et al. PSR J0030+0451 Mass and Radius from NICER Data and Implications for the Properties of Neutron Star Matter. *Astrophysical Journal Letters*, 887:L24, 2019. doi: 10.3847/2041-8213/ab50c5.

[16] T. E. Riley et al. A NICER View of the Massive Pulsar PSR J0740+6620 Informed by Radio Timing and XMM-Newton Spectroscopy. *Astrophysical Journal Letters*, 918:L27, 2021. doi: 10.3847/2041-8213/ac0a81.

[17] M. C. Miller et al. The Radius of PSR J0740+6620 from NICER and XMM-Newton Data. *Astrophysical Journal Letters*, 918:L28, 2021. doi: 10.3847/2041-8213/ac089b.

[18] D. Choudhury et al. A NICER View of the Nearest and Brightest Millisecond Pulsar: PSR J0437−4715. *Astrophysical Journal Letters*, 971:L20, 2024. doi: 10.3847/2041-8213/ad5a6f.

[19] E. Annala et al. Evidence for Quark-Matter Cores in Massive Neutron Stars. *Nature Physics*, 18:1143–1147, 2022. doi: 10.1038/s41567-022-01714-1.

[20] E. Fonseca et al. Refined Mass and Geometric Measurements of the High-Mass PSR J0740+6620. *Astrophysical Journal Letters*, 915:L12, 2021. doi: 10.3847/2041-8213/ac03b8.

[21] R. W. Romani et al. PSR J0952−0607: The Fastest and Heaviest Known Galactic Disk Pulsar. *Astrophysical Journal Letters*, 934:L17, 2022. doi: 10.3847/2041-8213/ac8007.

[22] K. Hebeler, J. M. Lattimer, C. J. Pethick, and A. Schwenk. Equation of State and Neutron Star Properties Constrained by Nuclear Physics and Observation. *Astrophysical Journal*, 773:11, 2013. doi: 10.1088/0004-637X/773/1/11.

References iv

[23] R. Abbott et al. Lattice QCD Constraints on the Equation of State of Dense Matter. *Physical Review D*, 109:034504, 2024. doi: 10.1103/PhysRevD.109.034504.

[24] G. Baym, C. Pethick, and P. Sutherland. The Ground State of Matter at High Densities: Equation of State and Stellar Models. *Astrophysical Journal*, 170:299, 1971. doi: 10.1086/151216.

[25] K. Hebeler. Nuclear Force Uncertainties and their Constraints on the Neutron Star Equation of State. *Physics Reports*, 890:1–48, 2021. doi: 10.1016/j.physrep.2020.08.009.

[26] I. Tews, J. Margueron, and S. Reddy. Critical Examination of Constraints on the Equation of State of Dense Matter Obtained from GW170817. *Physical Review C*, 98:045804, 2018. doi: 10.1103/PhysRevC.98.045804.

[27] P. Landry, R. Essick, and K. Chatziioannou. Nonparametric Constraints on Neutron Star Matter with Existing and Upcoming Gravitational Wave and Pulsar Observations. *Physical Review D*, 101:123007, 2020. doi: 10.1103/PhysRevD.101.123007.

[28] A. Kurkela, P. Romatschke, and A. Vuorinen. Cold Quark Matter. *Physical Review D*, 81:105021, 2010. doi: 10.1103/PhysRevD.81.105021.

[29] M. Ferreira and C. Providência. Neutron Star Properties from a Machine Learning Equation of State with Relativistic Mean Field Origins. *Physical Review D*, 110:063018, 2024. doi: 10.1103/PhysRevD.110.063018.

[30] Y. Lim and J. W. Holt. Bayesian Modeling of the Nuclear Equation of State for Neutron Star Tidal Deformabilities and GW170817. *European Physical Journal A*, 55:209, 2019. doi: 10.1140/epja/i2019-12917-9.